INDIAN JOURNAL OF SCIENCE AND TECHNOLOGY

RESEARCH ARTICLE

Performance Enhancement of THz Antenna with Reduced Size of Graphene Metasurface Unit Cell Structure Array

Nipun Sharma[1]*, **Amrit Kaur**[1]

1 Electronics and Communication Engineering Department Punjabi University, Patiala, Punjab, India

OPEN ACCESS

Received: 19-06-2023

Accepted: 01-10-2023

Published: 27-10-2023

Citation: Sharma N, Kaur A (2023) Performance Enhancement of THz Antenna with Reduced Size of Graphene Metasurface Unit Cell Structure Array. Indian Journal of Science and Technology 16(40): 3507-3514. https://doi.org/10.17485/IJST/v16i40.1502

* **Corresponding author**.

nipunharitash@gmail.com

Funding: None

Competing Interests: None

Published By Indian Society for Education and Environment (iSee)

ISSN
Print: 0974-6846
Electronic: 0974-5645

Abstract

Objectives: To design a metasurface layer of graphene unit cells with reduced surface area by incorporating different geometry of unit cell. **Methods:** The metasurface layer in the form of unit cell array is traditionally made of very simple geometry like square unit cell to limit design complexity. However, if the unit cell structure geometry is changed to triangular shape, it reduces the total surface area of the metasurface layer, thereby saving the graphene material. The proposed design is not only reduces the size of the metasurface layer of THz antenna but also enhances the performance of the antenna. **Findings:** The single square unit cell structure has 337.46 μm^2 area and an array of 9 x 9 such unit cells consume 27334.26 μm^2area. On the other hand, a single triangular unit cell design is 123.94 μm^2 and an array of 9 x 9 such unit cells consume only 10039.14 μm^2 area which is a saving of 63.35 % metasurface material. **Novelty:** The proposed antenna design in the paper compares the existing designs for better bandwidth, better return loss and reduction in the total surface area utilized by the metasurface layer and delivers a better performance.

Keywords: Microstrip Patch Antenna; Thz Antenna; Metasurface; Unit Cell Structure; Wide Band Antenna

1 Introduction

Metasurface based antennas are gaining a lot of popularity, owing to their ability to work in THz range and extremely small designs. A lot of research is being carried out in controlling antenna radiation pattern (beam steering) through means like photons [(1)], and multi-directional beaming is also obtained by using metasurface antennas [(2)].Other antenna parameters like bandwidth are gain are being enhanced using AIRP-m metasurfaces [(3)]. Designs of MIMO antennas are optimized for higher bandwidths for 6G communications [(4)] and isolation is achieved using metasurfaces [(5)]. The metasurface material is yet another area where a lot of experimentation is performed, textile based wearable antenna designs are being explored for body area networks [(6)]. These metasurface based antennas are finding a lot of applications on on-chip devices as well [(7)]. Metasurfaces are deployed in large gamut of antenna applications like

polarization control[8,9], isolation improvement[10], substrate implementation[11] and size reduction for analyzing characteristics mode analysis (CMA)[12]. An interesting area is the ultra-wide-band (UWB) application of metasurface antenna by the Antipodal Vivaldi antennas for high gain[13]. Metasurfaces have been able to provide electromagnetic invisibility to the antennas also[14]. A detailed study of the materials, mechanisms and meta devices suggest that control of light, wave, electricity and heat has resulted in a lot of progressives development in the field of communication[15]. Some vivid applications like graphene based solar absorption prediction is also found in the literature[16]. Graphene is a preferred choice of metasurface layer to design THz antennas for applications like dual frequency polarization[17], mmWave applications[18] and resonators etc[19]. This paper also tries to explore the wide band application of metasurface based antennas and reducing the effective size of the metasurface layer of the antenna at the same time.

1.1 Research Gap

The literature study and review in Section 1 clearly suggests that the area of implementing metasurfaces in the antenna is still a very evolving field and a lot of simulation-based experimentation is done. This experimentation surely discusses the implementation of the metasurface layers on the patch antenna design[20], but lack the optimization part. Optimization can be achieved by calibrated design of the metasurface layer for proper geometry to save metasurface material. The existing antenna designs gives small bandwidths and, in some designs, metasurface layer is missing. These gaps are addressed in the proposed work presented in the paper and the comparison of the results is shown in the results section.

1.2 Design Model

The design of the antenna is governed by certain equations that result in dimensions of the antenna. The design of microstrip patch antenna consists of a substrate and ground plane. On top of the substrate is the patch antenna. Then, on top of the patch antenna is the metasurface layer. The metasurface layer consists of the unit cell arrays. The substrate material is Silicon dioxide SiO_2. The ground plane and the patch antenna material are gold. The metasurface layer is made up of graphene. Two variations of this design are made, tested and compared in this paper.

1.3 Design-1

First design consists of metasurface layer of square unit cells of graphene. The dimensions of the 1st antenna are tabulated in Table 1 and the top view of the antenna is shown in Figure 1. The dimensional top view of the individual square unit cell is shown in Figure 2.

Table 1. Dimensions of antenna design with square unit cell array of 9 X 9

Name of the design parameter	Absolute Value	Unit (μm)
ls (length of substrate	216	μm
ws (width of substrate)	256	μm
g_he (ground height)	1	μm
s_he (substrate height)	26	μm
lp (length of patch)	120	μm
wp (width of patch)	160	μm
lf (length of feed)	108	μm
wf (width of feed)	54.78	μm
s_he1 (height of metasurface layer)	12	μm
d (side of unit cell	20	μm
r1 (radius of inner circle)	5	μm
sq (side of inner square)	4	μm
dis_x(metasurface layer displacement in x)	2	μm
dis_y(metasurface layer displacement in y)	22	μm
py (gap between unit cell in x)	4	μm
px (gap between unit cell in y)	4	μm

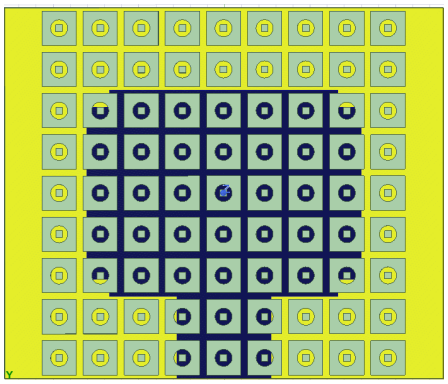

Fig 1. Antenna design with slotted patch and meta surface layer of square unit cells of 9 X 9 array

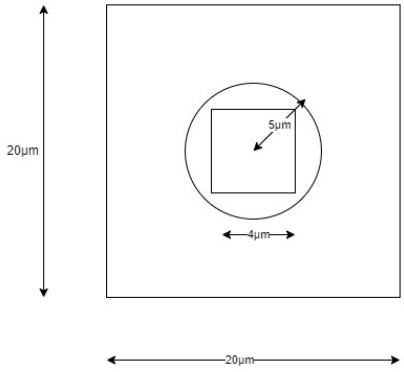

Fig 2. Unit Cell dimension/geometry of square shape

As the metasurface layer consists of a 9 X 9 array of square unit cells of dimensions as shown in Figure 2. It is important to calculate the total surface area of the metasurface layer to compare it with the 2nd design. According to the geometry the surface area of single unit cell is computed in Equation 1

$$\text{Effective Surface area of unit cell square is } \left(400\mu m^2 - 78.54\mu m^2 + 16\mu m^2\right) = 337.46\mu m^2 \quad (1)$$

The total surface area consumed by the metasurface unit cell array of 9 X 9 such unit cells is 27334.26 μm^2.

1.4 Design-2

Second design consists of metasurface layer of triangular unit cells of graphene. The dimensions of the 2nd antenna are tabulated in Table 2 and the top view of the antenna is shown in Figure 3. The dimensional top view of the individual square unit cell is shown in Figure 4.

Table 2. Dimensions of antenna design with triangular unit cell array of 9 X 9

Name of the design parameter	Absolute Value	Unit (μm)
ls (length of substrate	216	μm
ws (width of substrate)	256	μm
g_he (ground height)	1	μm
s_he (substrate height)	26	μm
lp (length of patch)	120	μm
wp (width of patch)	160	μm
lf (length of feed)	108	μm
wf (width of feed)	54.78	μm

Continued on next page

Table 2 continued		
s_he1 (height of metasurface layer)	12	μm
d (side of triangular unit cell	20	μm
r1 (radius of inside circle)	4	μm
sq (side of inside square)	1	μm
dis_x(metasurface layer displacement in x)	1	μm
dis_y(metasurface layer displacement in y)	22	μm
py (gap between unit cell in x)	4	μm
px (gap between unit cell in y)	4	μm

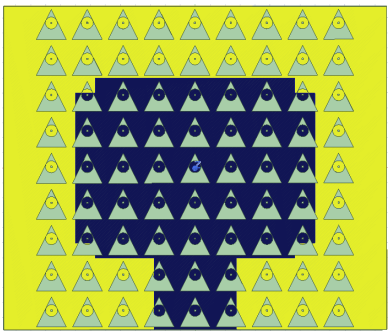

Fig 3. Antenna design with slotted patch and meta surface layer of triangular unit cells of 9 X9 array

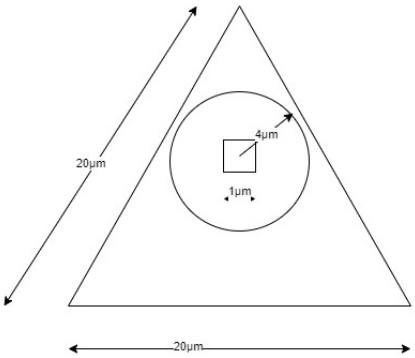

Fig 4. Unit cell dimensions/geometry of triangular shape.

As the metasurface layer consists of a 9 X 9 array of triangular unit cells of dimensions as shown in Figure 4. According to the geometry the surface area of single unit cell is computed in Equation 2.

$$\text{Effective Surface area of equilateral triangle unit cell is } \left(173.21\mu m^2 - 50.27\mu m^2 + 1\mu m^2\right) = 123.94\mu m^2 \quad (2)$$

The total surface area consumed by the metasurface unit cell array of 9 X 9 such unit cells is 10039.14 μm^2.

1.5 Evaluation of Performance Parameters

The simulation of the two designs of the antenna discussed in the above section is done in the Ansys Electronics Desktop 2021R1. To limit the scope of this paper, we have only discussed and compared the S_{11} parameters of the two designs of the antenna. It is explored extensively in the research [21]. It is defined as the ratio of output voltage of port 1 to the voltage going into the port 1 as shown in Equation 3.

$$S(11)\, or\ return\ loss = -10\, log(\frac{Returned\ Power}{Incident\ Power}) \quad (3)$$

It is also popularly known as the return loss (RL) in antenna terms and is a measure of the reflected energy of the antenna. It is expressed in decibel scale and minimum of -10db return is desired for optimized performance of the antenna.

2 Methodology

Parameters of antenna and unit cell structures are critical to obtain the desired resonance frequency using antenna equations. Some of the key parameters are discussed in this section Resonant Frequency: This is known as the primary operating frequency of the antenna. It is given by f_c, as shown in Equation 4. It depends on the electrical length of the antenna where the capacitive and the inductive reactance cancel each other.

$$f_c = \frac{c}{2L\sqrt{\in_o \in_r \mu_0}} \tag{4}$$

where c = speed of light, $\in_o$= permittivity of the free space, $\in_r$ = relative permittivity of the substrate, μ_0 = permeability of the free space Bandwidth: It is the known as the range of frequencies within which the antenna will radiate or receive EM energy. In terms of permittivity and dimension it is given by B as in Equation 5.

$$B \propto \frac{\in_r -1}{\varepsilon_r{}^2} \frac{W}{L} h \tag{5}$$

where W = width of the patch antenna, L = length of the patch antenna, h, height of the substrate Field Components: The Electric field value in 3-Dimensional space is given by The components E_θ and E_φ are given by Equation 6 and Equation 7 respectively.

$$E_\theta = \frac{\left[\sin \frac{kW}{2} \sin\theta \sin\varphi\right]}{\left[\frac{kW}{2} \sin\theta \sin\varphi\right]} \cdot \cos\left[\frac{kL}{2} \sin\theta \cos\varphi\right] \cos\varphi \tag{6}$$

$$E_\varphi = -\frac{\left[\sin \frac{kW}{2} \sin\theta \sin\varphi\right]}{\left[\frac{kW}{2} \sin\theta \sin\varphi\right]} \cdot \cos\left[\frac{kL}{2} \sin\theta \cos\varphi\right] \cos\theta \,\mathrm{si} \tag{7}$$

Where $k = \frac{2\pi}{\lambda}$

The following observations are made with respect to the constructional properties to the microstrip patch antennas. All of the parameters in a rectangular patch antenna design (L, W, h, permittivity) control the properties of the antenna.

Table 3. Variation of Patch Antenna Properties with Dimensions

Length	Width	Height of Substrate	Permittivity of Substrate
1. Inversely proportional of the resonant frequency 2. Inversely proportional to the permittivity of the substrate	1. Directly proportional to the bandwidth 2. Inversely proportional to the input impedance	1. Directly proportional to the bandwidth	1. Inversely proportional to the fringing fields 2. Inversely proportional to the bandwidth 3. Inversely proportional to the efficiency 4. Directly proportional to the impedance 5. Inversely proportional to the resonant frequency.

All the typical measurements of the proposed designs are in μm. The antenna parameters of design-1 are mentioned in Table 1 and antenna parameters of design-2 are mentioned in Table 2 . As far as the Simulation Setup is concerned, the simulation setup is done on Ansys Electronics Desktop 2021R1 and evaluated from 1 THz to 10 THz with a sweep frequency delta (δ) of 0.2 THz in 20 steps.

3 Results and Discussion

The S_{11} parameter plot of THz antenna with square unit cell metasurface array is shown in Figure 5. The resonant frequencies are observed and markers are placed at 4 points.

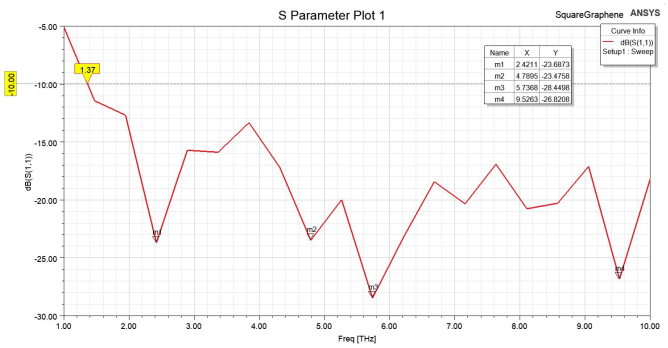

Fig 5. S11 parameter graph of antenna design with metasurface layer of square unit cells

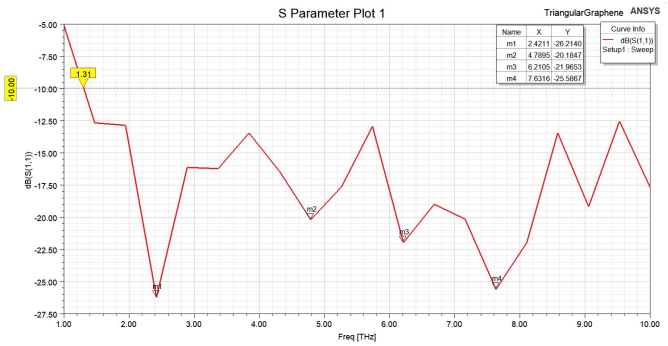

Fig 6. S11 parameter graph of antenna design with metasurface layer of triangular unit cells

The S_{11} parameter plot of THz antenna with triangular unit cell metasurface array is shown in Figure 6. The resonant frequencies are observed and markers are placed at 4 points.

The results of the entire simulation are exported in the csv file and the tabulation of the results of both the antennas are presented in Table 4. The Table 4 clearly shows that both antennas possess very high bandwidth as -10 dB bandwidth of antenna design 1 starts at 1.37 THz and antenna design 2 starts at 1.31 THz. After comparing the return loss values at 19 different frequencies, it is observed that both antenna designs are well suited for ultra-wide band applications. However, the interpretation of the results is presented in the conclusion section.

Table 4. Comparison of S11 parameters of two antenna designs with square and triangular unit cell geometry in metasurface layer

Antenna Design 1 with Rectangular Unit Cell metasurface array		**Antenna design 2 with Triangular Unit Cell metasurface array**	
Freq [THz]	S_{11} (in dB)	Freq [THz]	S_{11} (in dB)
1	-5.083258727(not in Bandwidth)	1	-5.070536451(not in Bandwidth)
1.473684211	-11.45481188	1.473684211	-12.67197575
1.947368421	-12.6934766	1.947368421	-12.86638773
2.421052632	-23.68725408	2.421052632	-26.21395126
2.894736842	-15.71369681	2.894736842	-16.1244147
3.368421053	-15.88670509	3.368421053	-16.23000239
3.842105263	-13.3392965	3.842105263	-13.45785404
4.315789474	-17.20801299	4.315789474	-16.47638593
4.789473684	-23.47582609	4.789473684	-20.18466231
5.263157895	-19.97626711	5.263157895	-17.61918556
5.736842105	-28.44981627	5.736842105	-12.94452373
6.210526316	-23.23229521	6.210526316	-21.96529455
6.684210526	-18.42592885	6.684210526	-18.98741886
7.157894737	-20.32927373	7.157894737	-20.44506834
7.631578947	-16.91768608	7.631578947	-25.58669717

Continued on next page

Table 4 continued

8.105263158	-20.75634496	8.105263158	-21.95256777
8.578947368	-20.2807081	8.578947368	-13.45686327
9.052631579	-17.10990193	9.052631579	-19.17276333
9.526315789	-26.82083878	9.526315789	-12.54082554
10	-18.14601052	10	-17.71946604

The results of the proposed work is compared with the existing designs in Table 5. The comparative analysis of the proposed antenna with the already designed antennas in the literature clearly shows that the improved bandwidth and better return loss is achieved. The Table 5 shows that the antenna design in [22] lacks metasurface layer and therefore gives only .371 THz of bandwidth and the antenna design in [23] has only single geometry of metasurface layer in the antenna design and gives 1.4 THz bandwidth. However, the proposed design in this paper has tested antenna design with two geometries of unit cells in the metasurface layer and suggests the triangular unit cell array for metasurface layer for better bandwidth (2.3684 THz (between 1st and 2nd resonant frequency)), return loss and reduction in size of metasurface layer.

Table 5. Performance Comparison of the proposed THz antenna structure with the existing structure

Parameters	[22] **Khan MAK et. al.**	[23] **Shubham A et.al.**	**Proposed Work**	**Observation of proposed work**
Patch Type	Various Shapes (Circular, Triangular)	Rectangular	Slotted Rectangular	Improved Bandwidth and less surface area in patch
Metasurface Layer	Not Present	Array of square unit cells	Array of square unit cells, Array of Triangular Unit cells	Improved Bandwidth and new triangular unit cell array introduced in metasurface layer.
Bandwidth	.371 THz	1.4 THz	2.3684 THz (between 1st and 2nd resonant frequency)	Improved
S_{11} (return loss)	-15.4 to -48.85 dB (for different materials of patches)	-17.03 dB	-23.68 dB (for Design-1) -26.21 dB (for Design-2)	Improved

4 Conclusion

The antenna designs proposed in the paper give excellent bandwidth in the THz range. The -10dB bandwidth for S_{11} range of antenna design 1 (with the metasurface layer of square unit cells) starts from 1.37 THz and -10dB S_{11} range of antenna design with the metasurface layer of triangular unit cells starts from 1.31 THz. Therefore, there is an enhancement of 0.06 THz bandwidth with the antenna design of triangular unit cell graphene metasurface structure. Comparing Equation 1 and Equation 2, we conclude that the single square unit cell structure has 337.46 μm^2 area and an array of 9 x 9 such unit cells consume 27334.26 μm^2area. On the other hand, a single triangular unit cell design is 123.94 μm^2 and an array of 9 x 9 such unit cells consume only 10039.14 μm^2 area which is a saving of 63.35 % metasurface material.

4.1 Merits

The proposed antenna design of triangular unit cell metasurface array has several merits.

- It saves graphene material as it consumes 63.35 % less area than antenna design with square unit cell metasurface array. This savings can translate into more metasurface layers to be fabricated in bulk productions.
- The second merit of the antenna design with triangular unit cell metasurface array is the enhanced bandwidth of 0.06 THz.
- The third merit is better S_{11} parameter values at lower frequencies of the bandwidth i.e., from 1.31 THz to 3.84 THz as compared in the Table 3.

4.2 Demerits

The proposed antenna design of triangular unit cell metasurface array has an observed demerit that at higher frequencies of operating bandwidth, it underperforms as compared to the design with square graphene unit cells array in metasurface layer.

As for the future scope, these antenna designs can be evaluated for other performance parameters like polarization[24], radiation efficiency, directivity and beam-efficiency for 6G applications and medical applications etc. Another area where future research can be conducted is the application like polarization control and beam steering etc, of different possible metasurface materials in the metasurface layer of unit cell array. Finally, this research may also be taken as reference for the design of reconfigurable antennas.

References

1) Muqdad ZS, Alibakhshikenari M, Elwi TA, Hassain ZAA, Virdee BS, Sharma R, et al. Photonic controlled metasurface for intelligent antenna beam steering applications including 6G mobile communication systems. *AEU - International Journal of Electronics and Communications*. 2023;166:154652. Available from: https://doi.org/10.1016/j.aeue.2023.154652.
2) Kulkarni SS, Kumar A, Lambor AR, Nayak SK. Planar metasurface sub-reflector based dual-reflector antenna for multi-directional beaming. *AEU - International Journal of Electronics and Communications*. 2023;164:154621. Available from: https://doi.org/10.1016/j.aeue.2023.154621.
3) Mohanty A, Sahu S. Using AIRP-m metasurface as LWP for bandwidth and gain enhancement in designing compact quasi-TE dipole antenna for Wi-Fi applications. *AEU - International Journal of Electronics and Communications*. 2023;168:154726. Available from: https://doi.org/10.1016/j.aeue.2023.154726.
4) Saxena G, Chintakindi S, Kasim MA, Maduri PK, Awasthi YK, Kumar S, et al. Metasurface inspired wideband high isolation THz MIMO antenna for nano communication including 6G applications and liquid sensors. *Nano Communication Networks*. 2022;34:100421. Available from: https://doi.org/10.1016/j.nancom.2022.100421.
5) Singh A, Kumar A, Kanaujia BK. High gain and enhanced isolation MIMO antenna with FSS and metasurface. *Optik*. 2023;286:170982. Available from: https://doi.org/10.1016/j.ijleo.2023.170982.
6) Muhammad HA, Abdulkarim YI, Abdoul PA, Dong J. Textile and metasurface integrated wide-band wearable antenna for wireless body area network applications. *AEU - International Journal of Electronics and Communications*. 2023;169:154759. Available from: https://doi.org/10.1016/j.aeue.2023.154759.
7) Alibakhshikenari M, Virdee BS, Salekzamankhani S, Babaeian F, Ali SM, Iqbal A, et al. On-Chip Terahertz antenna array based on amalgamation of metasurface-inspired and artificial magnetic conductor technologies for next generation of wireless electronic devices. *AEU - International Journal of Electronics and Communications*. 2023;167:154684. Available from: https://doi.org/10.1016/j.aeue.2023.154684.
8) Deepti, Gangwar D, Singh S, Sharma AP, Singh SP, Lay-Ekuakille A. Design of polarization conversion metasurface for RCS reduction and gain improvement of patch antenna for Ku-band radar sensing applications. *Sensors and Actuators A: Physical*. 2022;333:113273. Available from: https://doi.org/10.1016/j.sna.2021.113273.
9) Behera BR, Mishra SK. A single-layered metasurface inspired broadband polarization reconfigurable printed monopole antenna for hybrid wireless applications. *AEU - International Journal of Electronics and Communications*. 2022;156:154405. Available from: https://doi.org/10.1016/j.aeue.2022.154405.
10) Puri V, Singh HS. Design of an isolation improved MIMO antenna using metasurface based absorber for wireless applications. *Optik*. 2022;259:168963. Available from: https://doi.org/10.1016/j.ijleo.2022.168963.
11) Devarapalli AB, Moyra T. Low cross polarized leaf shaped broadband antenna with metasurface as superstrate for sub 6 GHz 5 G Applications. *Optik*. 2023;282:170858. Available from: https://doi.org/10.1016/j.ijleo.2023.170858.
12) Bian C, Zhang Y, Lv D, Yan M, Zhou D, Song C. A compact dual-band filtering metasurface antenna based on characteristic mode analysis. *AEU - International Journal of Electronics and Communications*. 2023;163:154607. Available from: https://doi.org/10.1016/j.aeue.2023.154607.
13) Jaiswal PK, Bhattacharya R, Kumar A. A UWB Antipodal Vivaldi antenna with high gain using metasurface and notches. *AEU - International Journal of Electronics and Communications*. 2023;159:154473. Available from: https://doi.org/10.1016/j.aeue.2022.154473.
14) Vellucci S, Monti A, Barbuto M, Toscano A, Bilotti F. Progress and perspective on advanced cloaking metasurfaces: from invisibility to intelligent antennas. *EPJ Applied Metamaterials*. 2021;8:7. Available from: https://doi.org/10.1051/epjam/2020013.
15) Ali A, Mitra A, Aïssa B. Metamaterials and Metasurfaces: A Review from the Perspectives of Materials, Mechanisms and Advanced Metadevices. *Nanomaterials*. 2022;12(6):1027. Available from: https://doi.org/10.3390/nano12061027.
16) Parmar J, Patel SK, Katkar V. Graphene-based metasurface solar absorber design with absorption prediction using machine learning. *Scientific Reports*. 2022;12(1). Available from: https://doi.org/10.1038/s41598-022-06687-6.
17) Zhang J, Tao S, Yan X, Zhang X, Guo J, Wen Z. Dual-Frequency Polarized Reconfigurable Terahertz Antenna Based on Graphene Metasurface and TOPAS. *Micromachines*. 2021;12(9):1088. Available from: https://doi.org/10.3390/mi12091088.
18) Magno G, Caramia L, Bianco GV, Bruno G, D'orazio A, Grande M. Design of optically transparent metasurfaces based on CVD graphene for mmWave applications. *Scientific Reports*. 2023;13(1). Available from: https://doi.org/10.1038/s41598-023-31298-0.
19) Devapriya AT, Robinson S. Investigation on Metamaterial Antenna for Terahertz Applications. *Journal of Microwaves, Optoelectronics and Electromagnetic Applications*. 2019;18(3):377–389. Available from: https://doi.org/10.1590/2179-10742019v18i31577.
20) Suyog P, Dipak P. Parameter enhancement and size reduction of metasurface reflector loaded decagon antenna for wireless applications. *AEU - International Journal of Electronics and Communications*. 2023;162:154567. Available from: https://doi.org/10.1016/j.aeue.2023.154567.
21) Yi H, Mu Y, Han J, Li L. Broadband millimeter-wave metasurface antenna array with printed ridge gap waveguide for high front-to-back ratio. *Journal of Information and Intelligence*. 2023;1(1):11–22. Available from: https://doi.org/10.1016/j.jiixd.2022.09.001.
22) Khan MAK, Shaem TA, Alim MA. Graphene patch antennas with different substrate shapes and materials. *Optik*. 2020;202:163700. Available from: https://doi.org/10.1016/j.ijleo.2019.163700.
23) Shubham A, Samantaray D, Ghosh SK, Dwivedi S, Bhattacharyya S. Performance improvement of a graphene patch antenna using metasurface for THz applications. *Optik*. 2022;264:169412. Available from: https://doi.org/10.1016/j.ijleo.2022.169412.
24) Cui J, Zhao X, Sheng W. Low profile and broadband circularly polarized metasurface antenna based on nonuniform array. *AEU - International Journal of Electronics and Communications*. 2022;156:154386. Available from: https://doi.org/10.1016/j.aeue.2022.154386.